NeoRdRp: A comprehensive dataset for identifying RNA-dependent RNA polymerase of various RNA viruses from metatranscriptomic data

Shoichi Sakaguchi[1], Syun-ichi Urayama[2], Yoshihiro Takaki[3], Kensuke Hirosuna[4], Hong Wu[1], Youichi Suzuki[1], Takuro Nunoura[5], Takashi Nakano[1*], So Nakagawa[6*]

[1]Department of Microbiology and Infection Control, Faculty of Medicine, Osaka Medical and Pharmaceutical University

[2]Laboratory of Fungal Interaction and Molecular Biology (donated by IFO), Department of Life and Environmental Sciences, University of Tsukuba

[3]Super-cuttingedge Grand and Advanced Research (SUGAR) Program, Japan Agency for Marine-Earth Science and Technology (JAMSTEC)

[4]Medical School, Osaka Medical and Pharmaceutical University, Takatsuki, Japan

[5]Research Center for Bioscience and Nanoscience (CeBN), Japan Agency for Marine-Earth Science and Technology (JAMSTEC)

[6]Department of Molecular Life Science, Tokai University School of Medicine

[*]Address correspondence to:

tnakano@ompu.ac.jp (TNakano); so@tokai.ac.jp (SN)

Keywords

RNA virome, RNA-dependent RNA polymerase, hidden Markov model, metatranscriptome

Running headline: NeoRdRp for RdRp identification

Abstract

RNA viruses are distributed throughout various environments, and most RNA viruses have recently been identified by metatranscriptome sequencing. However, due to the high nucleotide diversity of RNA viruses, it is still challenging to identify novel RNA viruses from metatranscriptome data. To overcome this issue, we created a dataset of RNA-dependent RNA polymerase (RdRp) domains that are essential for all RNA viruses belonging to *Orthornavirae*. Genes with RdRp domains from various RNA viruses were clustered based on their amino acid sequence similarity. For each cluster, a multiple sequence alignment was generated, and a hidden Markov model (HMM) profile was created if the number of sequences was greater than three. We further refined the 426 HMM profiles by detecting the RefSeq RNA virus sequences and subsequently combined the hit sequences with the RdRp domains. As a result, a total of 1,182 HMM profiles were generated from 12,502 RdRp domain sequences, and the dataset was named NeoRdRp. Almost all NeoRdRp HMM profiles successfully detected RdRp domains, specifically in the UniProt dataset. Furthermore, we compared the NeoRdRp dataset with two previously reported methods for RNA virus detection using metatranscriptome sequencing data. Our methods successfully identified most of the RNA viruses in the datasets; however, some RNA viruses were not detected, as in the cases of the other two methods. The NeoRdRp can be repeatedly improved by adding new RdRp sequences and is applicable as a system for detecting various RNA viruses from diverse metatranscriptome data.

Introduction

Currently, many RNA viruses have been identified by deep sequencing of RNA from diverse environmental samples (i.e., metatranscriptome) (Shi et al., 2018; Sakaguchi et al., 2020; Orba et al., 2021). Indeed, various metatranscriptomic analyses have revealed that RNA viruses, similar to human infectious viruses, such as coronaviruses, orthomyxoviruses, and filoviruses, are present even in non-mammalian species, including fishes (Shi et al., 2018). However, identifying RNA virus-derived sequences from metatranscriptome data is challenging because of the low abundance of viral RNA in sequencing reads and the high nucleotide diversity among RNA viruses (Cobbin et al., 2021). Thus, we have developed a method of double-stranded RNA (dsRNA) sequencing named "fragmented and primer ligated dsRNA sequencing" (FLDS) to enrich the RNA virus sequences in the cellular transcriptome (Urayama et al., 2016, 2018; Hirai et al., 2021). Long dsRNAs are rare in eukaryotic cells; therefore, they are mainly derived from the genomes of dsRNA viruses or replicative intermediates of single-strand RNA (ssRNA) viruses (Kumar and Carmichael, 1998). Moreover, FLDS enables us to obtain entire dsRNA sequences, including both termi, and to reconstruct multi-segmented genomes of RNA viruses based on terminal sequence similarity (Urayama et al., 2016). Accordingly, FLDS can enrich potential RNA virus genomes even though their sequences are dissimilar to known RNA viruses. However, it remains difficult to conclude RNA viral genomes based on FLDS data if genes specific to RNA viruses were not found.

Viruses that utilize RNA as a genetic material form a monophyletic group named *Riboviria* based on taxonomy annotation by ICTV (International Committee on Taxonomy of Viruses, https://talk.ictvonline.org/). *Orthornavirae* is a major kingdom of *Riboviria* containing all the dsRNA and ssRNA viruses — but excluding retroviruses — which harbor RNA-dependent RNA polymerase (RdRp). RdRp genes can be used as markers for most

70 RNA viruses; however, their nucleotide and amino acid sequences vary greatly, and some of
71 them have been identified as fusion genes with other protein motifs (Černý et al., 2014; Wolf
72 et al., 2018; Koonin et al., 2020, 2021). Indeed, it is often challenging to identify RNA virus
73 genes, including the RdRp gene, even in the cases of the potentially complete viral genome
74 sequences obtained by FLDS based on a similarity search using BLAST (Basic Local
75 Alignment Search Tool) with major amino acid databases (e.g., nr database or RefSeq
76 database) (Jia and Gong, 2019; Urayama et al., 2020).

77 In RdRp domain sequences, there are eight conserved amino acid motifs; notably, the
78 sixth motif containing three amino acid residues, GDD, is highly conserved (Koonin, 1991).
79 Based on these RdRp sequence motifs, Wolf and his colleagues inferred the phylogeny of
80 4,617 RNA viruses (Wolf et al., 2018). However, the accuracy of the multiple alignment of
81 all RdRp amino acid sequences was disputed due to their diversity (Holmes and Duchêne,
82 2019; Wolf et al., 2019). Therefore, in order to obtain reliable multiple alignments of RdRp
83 sequences, it is necessary to create multiple sequence alignments for each group defined by a
84 shared high sequence similarity.

85 This study collected RdRp domain sequences from 23,410 RNA viruses and clustered
86 them based on their similarity to build 1,182 hidden Markov model (HMM) profiles. Since an
87 HMM profile is based on a multiple sequence alignment, it can identify distantly related
88 sequences more efficiently than a pairwise-based search (Mistry et al., 2021). Several
89 bioinformatics approaches using HMM have been devised to identify more distantly related
90 viruses, such as VirSorter2 (Guo et al., 2021) and RVDB-prot (Goodacre et al., 2018; Bigot
91 et al., 2019). Note that since those datasets were based on various proteins in RNA and DNA
92 viruses (Goodacre et al., 2018; Bigot et al., 2019), the protein motifs identified by these
93 programs are not necessarily specific to RNA viruses. Furthermore, this study analyzed RdRp
94 sequences of marine RNA viruses obtained by FLDS and revealed that our method

successfully detected RdRp domains more efficiently than the two approaches mentioned above (i.e., VirSorter2 and RVDB-prot). The RdRp construction bioinformatics pipeline and constructed RdRp dataset, including annotation, are publicly available online (https://github.com/shoichisakaguchi/NeoRdRp).

99 **Materials and Methods**

100 Data sets

101 A total of 4,620 amino acid sequences containing RdRp domains annotated by Wolf and his
102 colleagues (Wolf et al., 2018) were downloaded from the NCBI (National Center for
103 Biotechnology Information) GenBank database. Additionally, we obtained 18,790 amino acid
104 sequences of 4,239 RNA viruses from the NCBI Virus database
105 (https://www.ncbi.nlm.nih.gov/labs/virus/vssi/) on June 9, 2021. These datasets are referred
106 to as Wolf-RdRps and NCBI-RNA-virus in this study, respectively.

107 The UniProt Knowledgebase (UniProtKB) containing manually curated protein
108 sequences and functional information concerning 565,928 genes [UniProtKB Reviewed
109 (Swiss-Prot) 2021-05-11] (Boutet et al., 2016) was used to validate and annotate our dataset.
110 The gene ontology (GO) molecular function of RdRp genes was GO:0003968 (RNA-directed
111 5'-3' RNA polymerase activity). In the UniProtKB database, 1,027 out of 565,928 amino
112 acid sequences were categorized as GO:0003968; of these, 836 were validated as RdRp-
113 containing genes (Supplementary Table 1).

114 In addition, potential RNA virus genome sequences obtained from the marine
115 metatranscriptomic analysis by fragmented and primer ligated dsRNA sequencing (FLDS)
116 were used as a benchmark dataset (Urayama et al., 2018). This dataset contains 228 RdRp
117 domains in 1,143 potentially complete RNA virus genomes. For each genome, open reading
118 frames (ORFs) longer than 30 nucleotides (starting with any sense codon) were predicted
119 using ORFfinder version 0.4.3, with the following options: -ml 30 -s 2 (available at
120 https://www.ncbi.nlm.nih.gov/orffinder/).

121

122 Clustering based on amino acid sequence similarity

123 Amino acid sequences were clustered using the CD-HIT program version 4.7 (Li and Godzik,
124 2006; Fu et al., 2012) with the following criteria: a similarity threshold of 60% and word size
125 of 4. A multiple sequence alignment was generated using the L-INS-i program in MAFFT
126 version 7.450 (Katoh and Standley, 2013). To select regions with solid statistical evidence of
127 shared homology for each multiple sequence alignment by replacing an amino acid in the
128 uncertainty regions with a gap (-) using Divvier version 1.0, with the default parameters (Ali
129 et al., 2019). In the multiple sequence alignment, if five or more amino acid positions
130 followed by more than 25% of the sequences consisted of gaps, the region was defined as a
131 boundary between two different domains. Then, the multiple sequence alignment was split at
132 the boundary using our in-house script. Multiple alignments of amino acid sequences were
133 visualized using WebLogo version 3.7.8 with the following options: -c chemistry -U
134 probability (Crooks et al., 2004).
135
136 Creation of Hidden Markov Model (HMM) profiles
137 For each multiple sequence alignment, an HMM profile was built using hmmbuild, part of
138 the HMMER3 package version 3.1b2 (Eddy, 2011) with default parameters. All HMM
139 profiles were then compressed into an HMMER3 searchable database using hmmpress in the
140 HMMER3 package with default parameters.
141
142 HMM and BLAST search
143 All HMM searches with HMM profiles were carried out using the hmmsearch program from
144 the HMMER3 package with default parameters and three sequence threshold E-values: "-E
145 1E-10", "-E 1E-20" and "-E 1E-30". Two hits in a sequence with gaps of less than 500 amino
146 acid length were merged using BEDTools version 2.30.0 (Quinlan and Hall, 2010) with a
147 "merge -d 500" option (Supplementary Fig. 1). The BLASTp program from the BLAST+

148 software suite version 2.12.0 (Camacho et al., 2009) was used with "-evalue 1e-10," "-evalue
149 1e-20," and "-evalue 1e-30" options.
150
151 VirSorter2 and RVDB-prot
152 VirSorter2 (Guo et al., 2021) was used with the option "--include-groups RNA," targeting the
153 search group set to RNA viruses only. The HMM profiles obtained from Reference Viral
154 Protein DataBase (RVDB-prot) version 22.0 (Bigot et al., 2019) were used with the
155 hmmsearch program.
156
157 Computer resource
158 A workstation PC (CPU, Intel Core i9-7980XE 2.60 GHz; Memory, 128 GB; Storage 19 TB
159 SSD) with Linux OS (Ubuntu 18.04.6 LTS) was used for benchmarking each bioinformatics
160 program.

161 **Results**

162 Constructing RdRp HMM profiles

163 The schematic procedure for constructing the RdRp HMM profiles is illustrated in Fig. 1.
164 The details of datasets and software used for the analysis are described in Materials and
165 Methods. First, we obtained the amino acid sequences of 4,620 RdRp genes and those with
166 the RdRp domain selected by Wolf and his colleagues (named Wolf-RdRps) (Wolf et al.,
167 2018). Next, we clustered the 4,620 amino acid sequences based on their sequence
168 similarities and then obtained 3,190 clusters. Clusters containing more than three sequences
169 (262 clusters in total) were used for the HMM profile construction. For each cluster, the
170 amino acid sequences were aligned. Since genes including RdRp domain may contain
171 multiple other domains, unreliable regions in the multiple sequence alignments were replaced
172 with gaps. Then, in the multiple sequence alignment, if five or more amino acid positions
173 followed by more than 25% of the sequences consisted of gaps, the region was split there and
174 divided into two multiple alignments. Subsequently, a multiple sequence alignment
175 consisting of more than nine amino acids was defined as a domain. For each domain, an
176 HMM profile was created, and a total of 426 HMM profiles were obtained. The script for the
177 above-mentioned bioinformatics procedure is available at the website:
178 https://github.com/shoichisakaguchi/NeoRdRp.

179 Furthermore, we conducted comprehensive similarity searches using the 426 HMM
180 profiles with 18,790 amino acid sequences of 4,239 RefSeq RNA virus genomes downloaded
181 from NCBI Virus (named NCBI-RNA-Virus). A total of 7,463 viral amino acid sequences
182 were obtained through the HMM search. The obtained amino acid sequences were combined
183 with Wolf-RdRps, resulting in 12,502 amino acid sequences named "NeoRdRp-seq."
184 Applying the same procedure for HMM construction (1st round shown in Fig. 1), we
185 clustered the NeoRdRp-seq dataset based on amino acid sequence similarity, resulting in

186 1,092 clusters (including 8,516 sequences). Note that 2,753 clusters (including 3,986
187 sequences) containing fewer than three sequences for each were excluded from the HMM
188 profile construction. The 1,092 clusters were processed as the same procedures, and 1,182
189 domains were extracted. Fig. 2 shows an example of the domain clearly indicating the well-
190 conserved protein motifs, DxxxxD, GxxxTxxxN, and GDD (Koonin, 1991). For each
191 domain, an HMM profile was created, and the 1,182 HMM profiles in total were obtained,
192 which were named "NeoRdRp-HMM" and are available at
193 https://github.com/shoichisakaguchi/NeoRdRp.
194
195 Evaluating NeoRdRp-HMM and NeoRdRp-seq
196 To evaluate NeoRdRp-HMM and NeoRdRp-seq, the amino acid sequences and annotation
197 information obtained from the UniProtKB Reviewed database were used. The dataset
198 consisted of 565,928 amino acid sequences, including 836 genes with RdRp domains (see
199 Materials and Methods and Supplementary Table 1). With the 565,928 amino acid sequences
200 as queries, we conducted comprehensive searches using hmmsearch or BLASTp, targeting
201 NeoRdRp-HMM or NeoRdRp-seq, respectively, with three different threshold E-values: 1E-
202 10, 1E-20, and 1E-30. The resulting data are summarized in Supplementary Table 2, and the
203 recall and precision rates calculated from them are summarized in Table 1. For both methods
204 and datasets, the smaller the E-value, the fewer the number of true-positive and false-positive
205 hits there were. In general, NeoRdRp-seq identified more genes with RdRp domain with
206 more false-positive sequences than NeoRdRp-HMM. For example, with the E-value 1E-10
207 threshold, 813 and 824 out of 836 genes with RdRp domain, and 246 and 1,316 out of
208 564,418 non-RdRp genes were detected using the NeoRdRp-HMM and NeoRdRp-seq
209 datasets, respectively. Furthermore, our dataset could identify genes with RdRp domain from

210 various RNA viruses, whereas 12 genes with RdRp domain (1.4%) derived from nine
211 Birnaviridae, two Reoviridae, and one Paramyxoviridae were not identified.
212 We also annotated NeoRdRp-HMM profiles based on the UniProtKB annotation of
213 Gene Ontology (GO; molecular function) with an E-value 1E-10 threshold. Out of 1,182
214 HMM profiles, 1,012 were evaluated; each hit was scored 1 if "RNA-directed 5'-3' RNA
215 polymerase activity" (GO:0003968) was included, and 0 if excluded. We then calculated the
216 mean value of the scores for each NeoRdRp-HMM profile, as summarized in Supplementary
217 Table 3. The mean score of the profiles was 0.92, suggesting that most NeoRdRp-HMM
218 profiles annotated using the UniProtKB search were derived from the RdRp domain
219 sequences of RNA viruses. However, we also found that 13 HMM profiles (1.3%) had a
220 score of 0; RNA binding [GO:0003723], ATP binding [GO:0005524], helicase activity
221 [GO:0004386], mRNA methyltransferase activity [GO:0008174], and hydrolase activity
222 [GO:0016787] were shared among the seven HMM profiles. The results indicated that these
223 HMM profiles with a score of 0 detected proteins that interact with RNA but do not contain
224 RdRp domains.
225
226 Comparing RdRp identification
227 We benchmarked the ability of NeoRdRp-HMM and NeoRdRp-seq to identify RNA viruses
228 using potentially complete RNA virus genome and genome segment sequences obtained by
229 FLDS associated with marine RNA viromes (Urayama et al., 2018). The data comprised
230 1,143 nucleotide sequences. Among these, 112,108 open reading frames (ORFs) longer than
231 30 nucleotides (i.e., 10 amino acids) were obtained (see Materials and Methods),
232 including 228 sequences annotated as genes with RdRp domain. The data set of the translated
233 amino acid sequences was named FLDS-data.

234 Using the FLDS-data, we evaluated NeoRdRp-HMM and NeoRdRp-seq using
235 hmmsearch and BLASTp, respectively. First, NeoRdRp-HMM and NeoRdRp-seq were
236 compared with E-values of 1E-10, 1E-20, and 1E-30; 181, 138, and 123 genes encoding
237 RdRp domain were found by both methods, respectively (Supplementary Fig. 2).
238 Furthermore, with the 1E-10, 1E-20, and 1E-30 E-values, none, 5, and 2 RdRp domain
239 sequences were detected only by NeoRdRp-HMM, whereas 18, 27, and 21 RdRp domain
240 sequences were by NeoRdRp-seq, respectively. The difference in RdRp identification
241 between the two methods could be explained by the advantage of the HMM search in the
242 detection of diversified RdRp domain sequences and the lower coverage of the current HMM
243 models because of the requirement of at least three sequences to create a new reliable HMM
244 profile.
245 We then merged the results of the NeoRdRp-HMM and NeoRdRp-seq searches into
246 NeoRdRp. Since NeoRdRp-seq may detect large false-positive hits with a low E-value
247 threshold (Table 1), the threshold E-value of the BLASTp search with NeoRdRp-seq was
248 fixed at 1E-30 in this search. VirSorter2 (Guo et al., 2021) and hmmsearch with RVDB-prot
249 (Goodacre et al., 2018) were used for comparison. Note that since VirSorter2 only accepts
250 nucleotide sequences as an input file, the original 1,143 nucleotide sequences of the FLDS-
251 data were used for VirSorter2. First, with a threshold E-value 1E-10 of hmmsearch, we
252 analyzed the 228 genes with RdRp domain using the three methods and detected them as
253 follows: 68 by all three methods, 116 by NeoRdRp and RVDB-prot, one by NeoRdRp and
254 VirSorter2, three by RdRp-prot and VirSorter2, three only by NeoRdRp, 17 only by RVDB-
255 prot, and 20 were not detected by any methods (Fig. 3). Although all hits by NeoRdRp-HMM
256 were also identified by RVDB-prot (Supplementary Fig. 3), viral genomes detected only by
257 NeoRdRp were classified into the family *Flaviviridae, Reoviridae*, and unclassified ssRNA
258 positive-strand viruses based on HMM patterns and genomic structures. However, the viral

259 genomes that the three methods could not detect were recognized as members of *Reoviridae*
260 and *Megabirnaviridae* (Urayama et al., 2018).
261 We also found 13 possible RdRp-containing sequences in the FLDS-data that were
262 not annotated previously. According to the NeoRdRp-HMM annotation, 13 RdRp domain
263 sequences were similar to those of *Picovirnaviridae*, unclassified viruses, or unclassified
264 dsRNA viruses (Supplementary Table 4). The results suggested that our dataset is useful for
265 detecting RdRps in metatranscriptome data that have been overlooked with previously
266 published bioinformatic pipelines.
267 We also compared the computational time required to search for RNA viruses in
268 FLDS-data using the three methods (Table 2): hmmsearch using NeoRdRp-HMM and
269 BLASTp using NeoRdRp-seq took 1 min 2 sec and 2 min 56 sec, respectively (i.e., 3 min and
270 58 sec in total for the NeoRdRp search); hmmsearch using RVDB-prot took 7 min 11 sec;
271 and search using VirSorter took 11 min 45 sec. Furthermore, the database size required for
272 each analysis was 0.37 GB for NeoRdRp, 1.61 GB for RVDB-prot, and 11.3 GB for
273 VirSorter2 (Table 2). The results indicated that the NeoRdRp dataset required a smaller
274 computational capacity than the other methods tested.
275
276 **Discussion**
277 Nucleic acid contamination from DNA viruses, hosts, and environments is an issue when
278 analyzing RNA viromes. To overcome this issue, techniques to selectively extract and
279 sequence RNA virus-derived nucleic acids, such as the FLDS method (Urayama et al., 2016;
280 Hirai et al., 2021), have been developed. However, it is still challenging to eliminate all
281 contamination from the sequencing data. Thus, in this study, RdRp genes, which are the
282 hallmark of RNA viruses, were comprehensively obtained (NeoRdRp-seq), and HMM
283 profiles of RdRp domains were constructed based on amino acid similarity (NeoRdRp-

284 HMM) (Fig. 1). Using this dataset, we successfully obtained various genes encoding the
285 RdRp domain from the FLDS-data (Fig. 3), while those of some RNA viruses could not be
286 detected (Table 1 and Fig. 3). In addition, although NeoRdRp-seq could be utilized as a
287 complement to RdRp-HMM, a BLASTp search using NeoRdRp-seq generated a relatively
288 large number of false-positive hits (Table 1). This is because an RdRp domain is sometimes
289 encoded in a fusion gene, and NeoRdRp-seq includes non-RdRp domain sequences of such
290 fusion genes. To overcome this problem, repeating updates with additional RdRp sequences
291 is necessary. In principle, as the number of RdRp sequences increases, the number of clusters
292 used for HMM construction also increases, and subsequently, the detection power must
293 increase. We designed the pipeline used for the NeoRdRp-HMM to create enhanced HMM
294 profiles by incorporating newly detected RdRp sequences. The pipeline for HMM
295 construction is available on GitHub (https://github.com/shoichisakaguchi/NeoRdRp).
296 Therefore, users can modify NeoRdRp-HMM using their own sequences. Accordingly,
297 continuing to update NeoRdRp-HMM with successively identified RdRp sequences would
298 reduce undetected RdRp sequences and false-positive hits.
299 The NeoRdRp dataset was based only on genes containing RdRp domains. Our
300 approach has advantages in the accuracy of RNA virus identification from highly diversified
301 metatranscriptome data, particularly for the presence of known viruses is not expected.
302 Meanwhile, since the NeoRdRp cannot identify non-RdRp genes in RNA viruses, the
303 NeoRdRp dataset can be applied for RNA virus detection and annotation from
304 metatranscriptome data as the following research design; assemble of metatranscriptomic
305 data, subsequent ORF search for each contig, and RdRp domain identification of each ORF
306 using NeoRdRp-HMM. If more RNA virus sequences are required, further searches using
307 NeoRdRp-seq are expected, although it may produce more false-positive hits (Table 1 and
308 Supplementary Table S2) and the process is relatively computationally intensive (Table 2).

309 Based on the combination of these methods and their scores, we can identify contigs
310 containing RdRp domain, suggesting that they are derived from RNA viruses. Furthermore,
311 FLDS can identify multi-segmented genomes of RNA viruses based on terminal sequence
312 similarity (Urayama et al., 2016). Therefore, if one contig is found to contain an RdRp
313 domain, other contigs with a similar sequence on their either termini are strongly implied to
314 be derived from RNA viruses. Further, in these contigs, other viral genes could be detected
315 using other computational programs and datasets, including VirSorter2 and RVDB-prot.
316 In conclusion, the NeoRdRp can detect various RdRps with a high degree of accuracy
317 (Table 1 and Fig. 3), and the dataset is very compact compared to other methods for RNA
318 virome searches (Table 2). All sequence data, annotations, and bioinformatics pipelines are
319 available on GitHub (https://github.com/shoichisakaguchi/NeoRdRp). Furthermore, by
320 updating the NeoRdRp with new RdRp sequences, it will be possible to find more RdRp
321 sequences with higher accuracy levels from various metatranscriptome data, which may
322 become an essential technique for discovering unknown RNA viruses.
323

324 **Acknowledgments**

325 This work was supported by KAKENHI Grant-in-Aid for Scientific Research (C) 20K06775
326 (to S.S. and S.N.); Early-Career Scientists 20K15685 (to S.S.); Challenging Research
327 (Pioneering) 18H05368 (to S.U., Y.T., and T.Nunoura); and Scientific Research on
328 Innovative Areas 16H06429 (to S.U. and S.N.), 16K21723 (to S.U. and S.N.), 16H06437 (to
329 S.U.), 19H04843 (to S.N.); and by AMED under grant numbers JP19fm0208009 (to S.U.),
330 JP20wm0325004 (to S.U.), and JP21wm0325004 (to S.U. and S.N.). The computing
331 resources were partially supported by the NIG supercomputer at the ROIS National Institute
332 of Genetics, Japan, and SHIROKANE at the Human Genome Center, the Institute of Medical
333 Science, the University of Tokyo, Japan.

334 **References**

335 Ali, R. H., Bogusz, M., and Whelan, S. (2019). Identifying Clusters of High Confidence
336 Homologies in Multiple Sequence Alignments. Mol. Biol. Evol. 36, 2340–2351.
337 Bigot, T., Temmam, S., Pérot, P., and Eloit, M. (2019). RVDB-prot, a reference viral
338 protein database and its HMM profiles. F1000Res. 8, 530.
339 Boutet, E., Lieberherr, D., Tognolli, M., Schneider, M., Bansal, P., Bridge, A. J., et al.
340 (2016). UniProtKB/Swiss-Prot, the Manually Annotated Section of the UniProt
341 KnowledgeBase: How to Use the Entry View. Methods Mol. Biol. 1374, 23–54.
342 Černý, J., Černá Bolfíková, B., Valdés, J. J., Grubhoffer, L., and Růžek, D. (2014).
343 Evolution of tertiary structure of viral RNA dependent polymerases. PLoS One 9,
344 e96070.
345 Christiam, C., Coulouris, G., Avagyan, V., Ma, N., Papadopoulos, J., Bealer, K., and
346 Madden, T.L. (2009). BLAST+: Architecture and Applications. BMC Bioinformatics 10,
347 421.
348 Cobbin, J. C., Charon, J., Harvey, E., Holmes, E. C., and Mahar, J. E. (2021). Current
349 challenges to virus discovery by meta-transcriptomics. Curr. Opin. Virol. 51, 48–55.
350 Crooks, G. E., Hon, G., Chandonia, J.-M., and Brenner, S. E. (2004). WebLogo: a
351 sequence logo generator. Genome Res. 14, 1188–1190.
352 Eddy, S. R. (2011). Accelerated Profile HMM Searches. PLoS Comput. Biol. 7,
353 e1002195.
354 Fu, L., Niu, B., Zhu, Z., Wu, S., and Li, W. (2012). CD-HIT: accelerated for clustering
355 the next-generation sequencing data. Bioinformatics 28, 3150–3152.
356 Goodacre, N., Aljanahi, A., Nandakumar, S., Mikailov, M., and Khan, A. S. (2018). A
357 Reference Viral Database (RVDB) To Enhance Bioinformatics Analysis of High-

358 Throughput Sequencing for Novel Virus Detection. mSphere 3.
359 doi:10.1128/mSphereDirect.00069-18.
360 Guo, J., Bolduc, B., Zayed, A. A., Varsani, A., Dominguez-Huerta, G., Delmont, T. O., et
361 al. (2021). VirSorter2: a multi-classifier, expert-guided approach to detect diverse DNA
362 and RNA viruses. Microbiome 9, 37.
363 Hirai, M., Takaki, Y., Kondo, F., Horie, M., Urayama, S.-I., and Nunoura, T. (2021).
364 RNA Viral Metagenome Analysis of Subnanogram dsRNA Using Fragmented and
365 Primer Ligated dsRNA Sequencing (FLDS). Microbes Environ. 36.
366 doi:10.1264/jsme2.ME20152.
367 Holmes, E. C., and Duchêne, S. (2019). Can Sequence Phylogenies Safely Infer the
368 Origin of the Global Virome? MBio 10. doi:10.1128/mBio.00289-19.
369 Jia, H., and Gong, P. (2019). A Structure-Function Diversity Survey of the RNA-
370 Dependent RNA Polymerases From the Positive-Strand RNA Viruses. Front. Microbiol.
371 10, 1945.
372 Katoh, K., and Standley, D. M. (2013). MAFFT multiple sequence alignment software
373 version 7: improvements in performance and usability. Mol. Biol. Evol. 30, 772–780.
374 Koonin, E. V. (1991). The phylogeny of RNA-dependent RNA polymerases of positive-
375 strand RNA viruses. J. Gen. Virol. 72 (Pt 9), 2197–2206.
376 Koonin, E. V., Dolja, V. V., Krupovic, M., and Kuhn, J. H. (2021). Viruses defined by
377 the position of the virosphere within the replicator space. Microbiol. Mol. Biol. Rev.,
378 e0019320.
379 Koonin, E. V., Dolja, V. V., Krupovic, M., Varsani, A., Wolf, Y. I., Yutin, N., et al.
380 (2020). Global Organization and Proposed Megataxonomy of the Virus World.
381 Microbiol. Mol. Biol. Rev. 84. doi:10.1128/MMBR.00061-19.

382 Kumar, M., and Carmichael, G. G. (1998). Antisense RNA: function and fate of duplex
383 RNA in cells of higher eukaryotes. Microbiol. Mol. Biol. Rev. 62, 1415–1434.
384 Li, W., and Godzik, A. (2006). Cd-hit: a fast program for clustering and comparing large
385 sets of protein or nucleotide sequences. Bioinformatics 22, 1658–1659.
386 Mistry, J., Chuguransky, S., Williams, L., Qureshi, M., Salazar, G. A., Sonnhammer, E.
387 L. L., et al. (2021). Pfam: The protein families database in 2021. Nucleic Acids Res. 49,
388 D412–D419.
389 Orba, Y., Matsuno, K., Nakao, R., Kryukov, K., Saito, Y., Kawamori, F., et al. (2021).
390 Diverse mosquito-specific flaviviruses in the Bolivian Amazon basin. J. Gen. Virol. 102.
391 doi:10.1099/jgv.0.001518.
392 Quinlan, A. R., and Hall, I. M. (2010). BEDTools: a flexible suite of utilities for
393 comparing genomic features. Bioinformatics 26, 841–842.
394 Sakaguchi, S., Nakagawa, S., Mitsuhashi, S., Ogawa, M., Sugiyama, K., Tamukai, K., et
395 al. (2020). Molecular characterization of feline paramyxovirus in Japanese cat
396 populations. Arch. Virol. 165, 413–418.
397 Shi, M., Zhang, Y.-Z., and Holmes, E. C. (2018). Meta-transcriptomics and the
398 evolutionary biology of RNA viruses. Virus Res. 243, 83–90.
399 Urayama, S.-I., Takaki, Y., Hagiwara, D., and Nunoura, T. (2020). dsRNA-seq Reveals
400 Novel RNA Virus and Virus-Like Putative Complete Genome Sequences from
401 Hymeniacidon sp. Sponge. Microbes Environ. 35. doi:10.1264/jsme2.ME19132.
402 Urayama, S.-I., Takaki, Y., Nishi, S., Yoshida-Takashima, Y., Deguchi, S., Takai, K., et
403 al. (2018). Unveiling the RNA virosphere associated with marine microorganisms. Mol.
404 Ecol. Resour. 18, 1444–1455.

405 Urayama, S.-I., Takaki, Y., and Nunoura, T. (2016). FLDS: A Comprehensive dsRNA
406 Sequencing Method for Intracellular RNA Virus Surveillance. Microbes Environ. 31, 33–
407 40.
408 Wolf, Y. I., Kazlauskas, D., Iranzo, J., Lucía-Sanz, A., Kuhn, J. H., Krupovic, M., et al.
409 (2018). Origins and Evolution of the Global RNA Virome. MBio 9.
410 doi:10.1128/mBio.02329-18.
411 Wolf, Y. I., Kazlauskas, D., Iranzo, J., Lucía-Sanz, A., Kuhn, J. H., Krupovic, M., et al.
412 (2019). Reply to Holmes and Duchêne, "Can Sequence Phylogenies Safely Infer the
413 Origin of the Global Virome?": Deep Phylogenetic Analysis of RNA Viruses Is Highly
414 Challenging but Not Meaningless. MBio 10. doi:10.1128/mBio.00542-19.

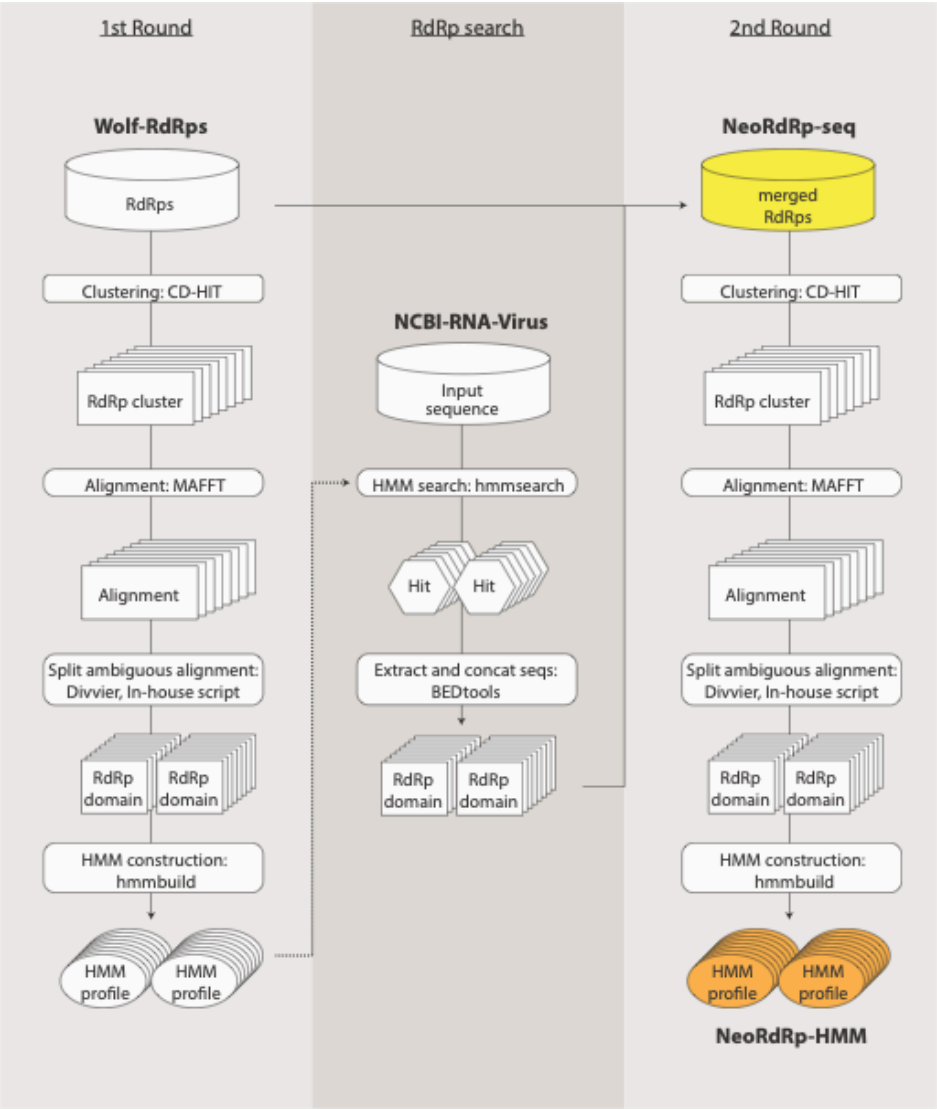

Fig. 1. A schematic workflow of NeoRdRp-HMM construction

(1st Round, left) Amino acid sequences containing RdRp domains in the Wolf-RdRps data were clustered based on similarity. For each cluster, a multiple sequence alignment was constructed and processed to create HMM profiles. (RdRp search, middle) The HMM profiles were used to detect the RdRp domain of amino acid sequences in the NCBI-RNA-Virus data. (2nd Round, right) The detected RdRp domain sequences were merged with the Wolf-RdRps data, which were clustered and processed to create HMM profiles for RdRp detection. The dataset names used in this study are in bold. Yellow, NeoRdRp-seq; orange, NeoRdRp-HMM.

Fig. 2. An example of a multiple sequence alignment of amino acid sequences including RdRp domain.

The multiple sequence alignment of the HMM profile of 1981.alnta.divvy_RDRP_0.25_923-1375 (including seven sequences) was visualized using Weblogo software. The height represents the probability at each site, and the width is proportional to the number of sequences. Underlines in red indicate the well-conserved DxxxxD, GxxxTxxxN, and GDD motifs in RdRp domain at positions 192–197, 258–266, and 303–305, respectively.

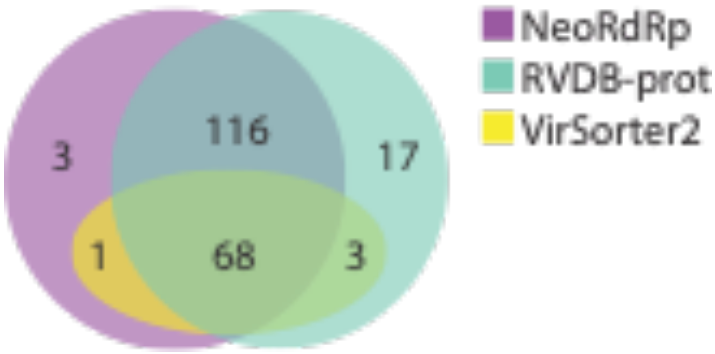

Fig. 3. Venn diagram of three different methods for identifying RNA viruses. Annotated marine metatranscriptome data were searched using NeoRdRp (NeoRdRp-HMM and NeoRdRp-seq), RVDB-prot, and VirSorter2. The number in each region indicates the number of hits by the method(s); for example, three were found only in NeoRdRp. Purple, NeoRdRp (NeoRdRp-HMM and NeoRdRp-seq); green, RVDB-prot; yellow, VirSorter2.

439 **Table 1. Recall and precision rates of NeoRdRp-HMM or NeoRdRp-seq searches for**

440 **each E-value threshold.**

	E-value ≤ 1E-10		E-value ≤ 1E-20		E-value ≤ 1E-30	
	Recall (%)	Precision (%)	Recall (%)	Precision (%)	Recall (%)	Precision (%)
NeoRdRp-HMM	97.2	76.8	96.8	84.8	96.2	85.0
NeoRdRp-seq	98.6	38.5	98.2	47.7	98.1	48.4
NeoRdRp	98.6	37.9	98.2	47.7	98.1	48.4

441

442 **Table 2. Database size and processing time of three methods for searching for RNA**

443 **viruses in FLDS data.**

Data	Tool	Database Type	Database Size (GB)	Speed
NeoRdRp-HMM/ NeoRdRp-Seq	hmmsearch/ BLASTp	HMM/ blast	0.36/ 0.02	1 min 2 sec/ 2 min 56 sec
RVDB-prot	hmmsearch	HMM	1.61	7 min 11 sec
VirSorter2	VirSorter2	VS2	11.13	11 min 45 sec

444

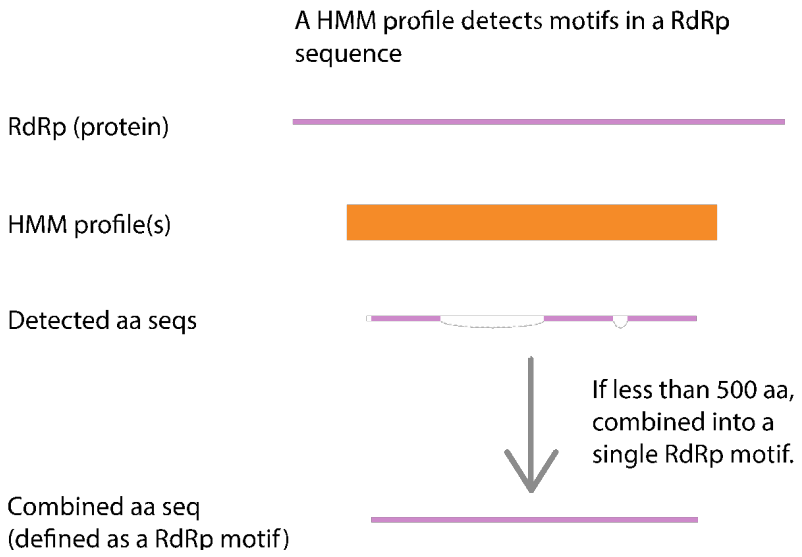

Supplementary Figure 1. Defining an RdRp domain.

When the detected sequence distance was less than 500 amino acid length in the hmmsearch results, we regarded them as a single region as a domain.

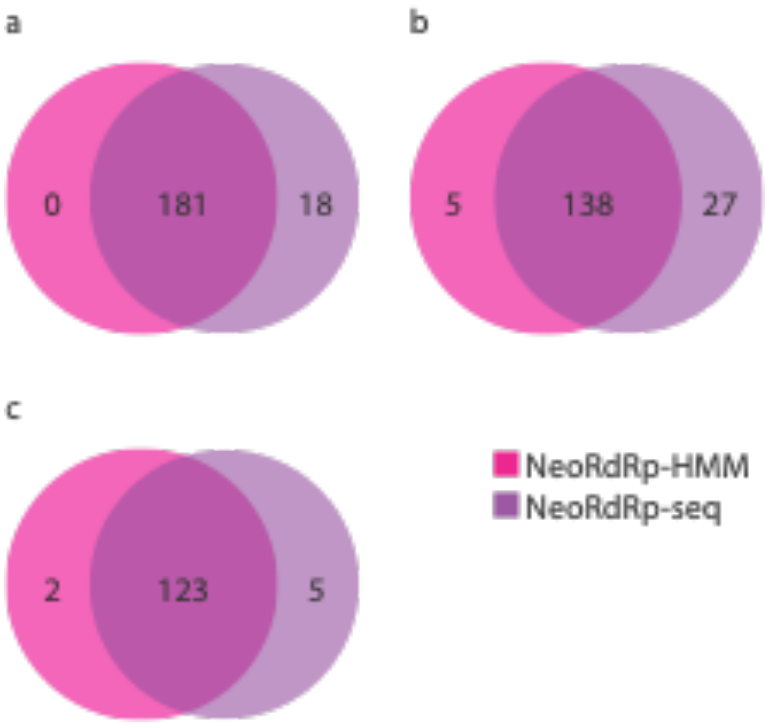

Supplementary Figure 2. Comparison of NeoRdRp-HMM and NeoRdRp-seq. NeoRdRp-HMM and NeoRdRp-seq with an E-values of (a) 1E-10, (b) 1E-20, and (c) 1E-30 were compared. Pink, NeoRdRp-HMM; purple, NeoRdRp-seq.

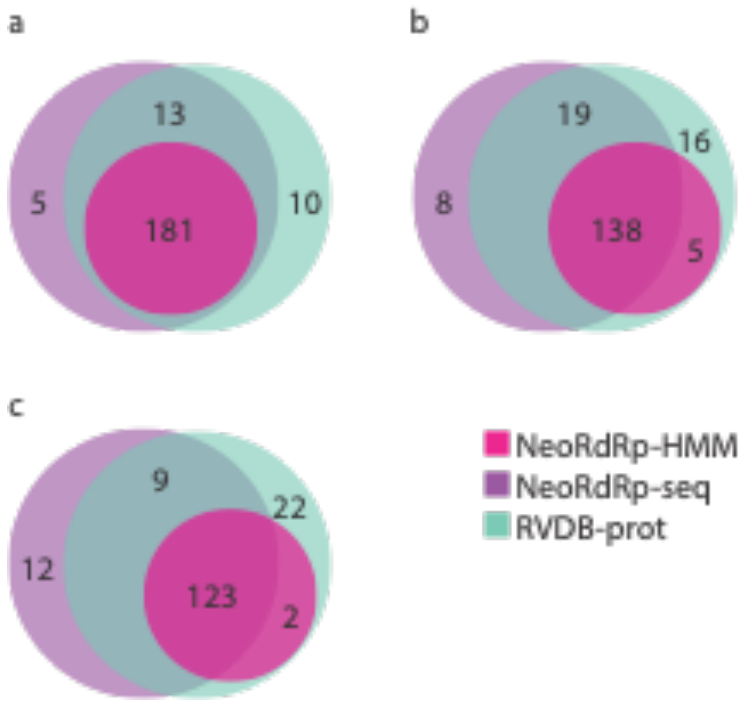

Supplementary Figure 3. Comparison of NeoRdRp-HMM and RVDB-prot.

NeoRdRp-HMM and NeoRdRp-seq with E-values of (a) 1E-10, (b) 1E-20 and (c) 1E-30 were compared. Pink, NeoRdRp-HMM; purple, NeoRdRp-seq; green, RVDB-prot.

Supplementary Table 1. 836 RdRp genes in the UniProt KB database.

(provided as an Excel File)

Supplementary Table 2. NeoRdRp-HMM or NeoRdRp-seq searches for each E-value threshold.

(provided as an Excel File)

Supplementary Table 3. Summary of the scores for each NeoRdRp-HMM profile.

(provided as an Excel File)

469 **Supplementary Table 4. Unannotated RdRps in metatranscriptome data detected by**

470 **NeoRdRp.**